Forward propagation of uncertainty and sensitivity analysis in an integral oil-gas plume model

Shitao Wang
Advisor: Mohamed Iskandarani
Committee members: Ashwanth Srinivasan, Tamay Özgökmen

Rosenstiel School of Marine and Atmospheric Science
Meteorology and Physical Oceanography

Outline

Introduction

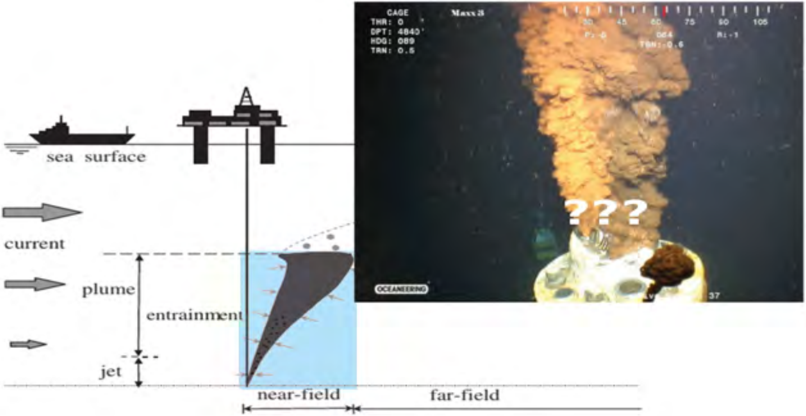

Motivation:

- Measurements in the deep ocean (*Deepwater Horizon*: 1500m) are extremely difficult.
- Uncertainties exist in many model parameters and initial conditions.
  ⇒ Uncertainty Quantification (UQ) framework is needed.

Introduction

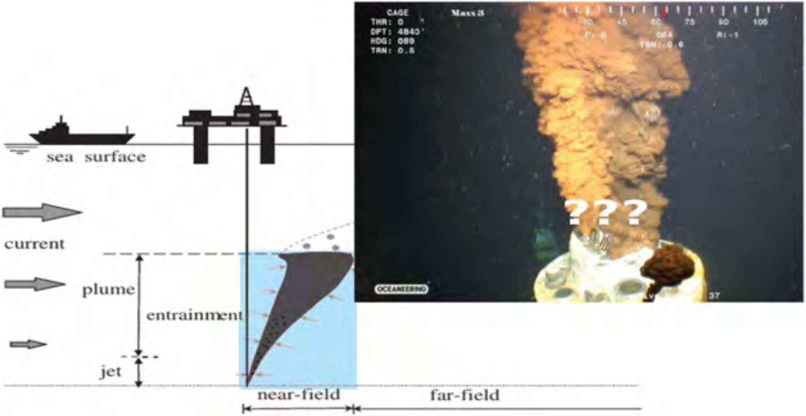

Goal:

Development, validation and application of UQ tools to an oil plume problem.

- Uncertainty propagation: input PDF ⇒ output PDF.
- Sensitivity analysis: identify the principle contributor to the output uncertainties.

Outline

Plume dynamics simulation

What is the near-field oil/gas plume predict?

A major role of the plume model is to provide initial conditions to its far-field counterparts.
In stratification-dominated plumes, intrusion dynamics must be modeled to the end of the plume-dominated region (Scott Socolofsky,E. Eric Adams,Øistein Johansen).

Simulating:

- Turbulent entrainment.
- Buoyant detrainment.
- 3-Phase flow (dissolution).

Predicting:

- The depth of the subsurface intrusion.
- The gas mass flux as a function of depth.

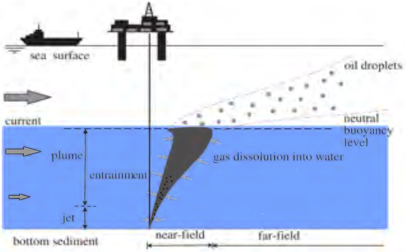

Figure 1 : Modified from Li Zheng et al. 2003

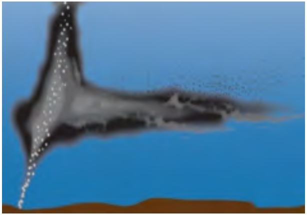

Figure 2 : Modified from Socolofsky 2012

Plume dynamics simulation

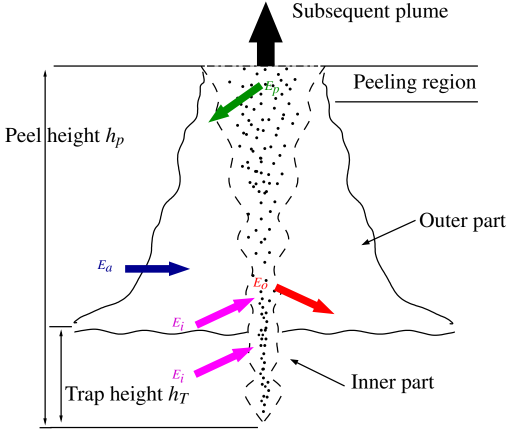

Inner plume formation

- Initial buoyancy and momentum drive an upward inner plume.
- Turbulent mixing entrains ambient fluid into inner plume.
- Heavier deep water is lifted to the lighter shallow water.
- A downward moving outer plume forms.
- A fraction of gas/oil continues to rise causing plume to restart.

Plume dynamics simulation

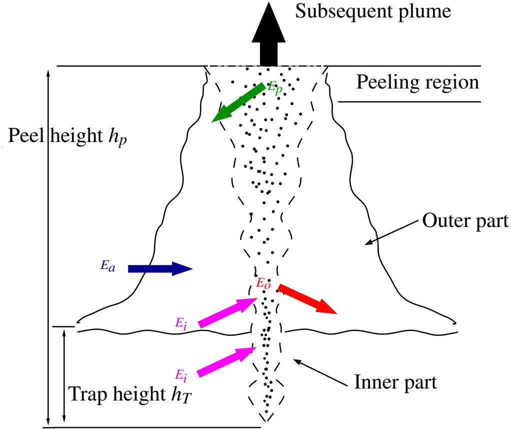

Inner plume formation

- Initial buoyancy and momentum drive an upward inner plume.
- Turbulent mixing entrains ambient fluid into inner plume.
- Heavier deep water is lifted to the lighter shallow water.
- A downward moving outer plume forms.
- A fraction of gas/oil continues to rise causing plume to restart.

Outer plume formation

- Turbulent mixing generates two new entrainment fluxes.
- Outer plume will be halted by the ambient stratification.
- Neutral buoyancy layer: ambient density = plume density.

Plume dynamics simulation

Why integral plume model?

- The simulation of deep water oil spill is very challegenging due to the turbulent, multi-phase and multi-scale nature of the flow.
- The detailed simulation of the mixing between the rising oil/gas plume and the ensuing three-way entrainment would require long computational times.
- An integral model is a good compromise because we are interested in the bulk quantities instead of detailed turbulent mixing.
- The results from integral model have been validated against lab/field experiments and numerical simulations (Asaeda and Imberger, 1993; Buscaglia et al., 2002; Johansen et al., 2003).

Outline

Integral plume model (Socolofsky et al. 2008)

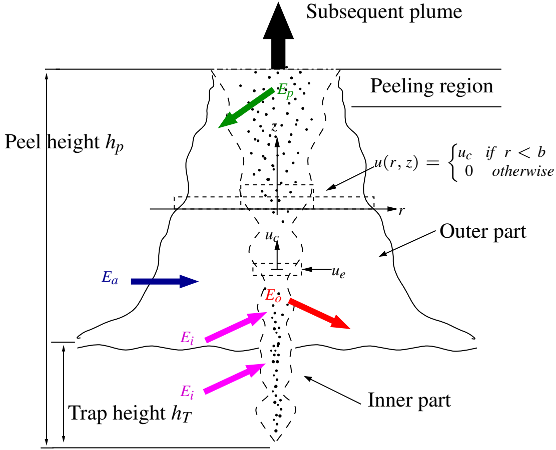

Model descriptions

- Stratification dominated (Camilli et al. 2010, Socolofsky et al. 2011).
- Double-plume approach (Socolofsky et al. 2008).

3D PDEs $\Rightarrow$ 1D ODEs:

- A time independent axisymmetric mean flow.
- Self-similarity of the mean flow profile.
- Turbulent entrainment parameterization.

The resulting 1D ODEs enforce well-established conservation laws.

Integral plume model (Socolofsky et al. 2008)

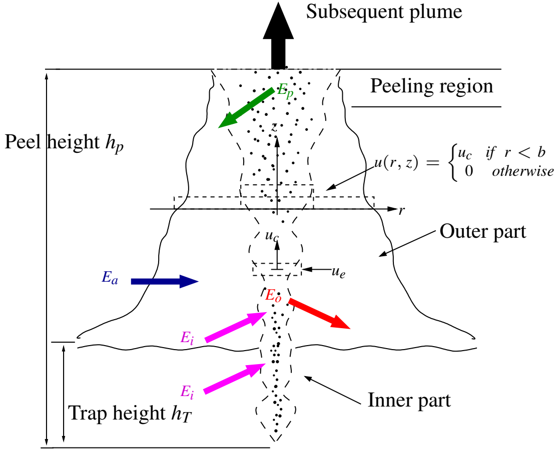

Model descriptions

- Stratification dominated (Camilli et al. 2010, Socolofsky et al. 2011).
- Double-plume approach (Socolofsky et al. 2008).

3D PDEs $\Rightarrow$ 1D ODEs:

- A time independent axisymmetric mean flow.
- Self-similarity of the mean flow profile.
- Turbulent entrainment parameterization.

The resulting 1D ODEs enforce well-established conservation laws.

Primary processes. (Crounse et al. 2007)

- Buoyancy forces acting upon the oil, gas and seawater.
- Dissolution of the gas bubbles.
- Turbulent entrainment.
- Buoyant detrainment/peeling.

Outline

Identifying Uncertainty Sources

Model input:

Parameters	*Deepwater Horizon* values
Release depth	1500 m
Pressure	CTD(R/V Brooks McCall at Station B54)
Salinity	CTD(R/V Brooks McCall at Station B54)
Ambient temperature	CTD (R/V Brooks McCall at Station B54)
Gas and oil temperature	37°C
Diameter of Riser	0.53 m
Oil density	858 kg/m^3
Gas composition	[methane, ethane, propane] [0.875, 0.081, 0.044]
Gas to oil ratio	
Flow rate	
Entrainment parameters	⇒ Uncertain parameters
Mass flux of oil of different droplet sizes	
Mass flux of gas of different bubble sizes	

Table 1 : Summary of DWH initial conditions (Lefebvre,1988; Bhaumik,2005; Valentine et al., 2010; Reddy et al., 2012).

- We focus on 6 parameters that strongly influence the evolution of buoyancy in the plume.
- We need to reduce the number of uncertain parameters from a practical point of view.

Characterizing the uncertain parameters

UQ requirements

- Uncertainty described via a probability density function (PDF) for each parameter.
- Lab or field data is insufficient to build an empirical input PDF.
- Use available data to identify the range of the uncertain parameters.
- Their distribution is assumed uniform within this range.

Characterizing the uncertain parameters

UQ requirements

- Uncertainty described via a probability density function (PDF) for each parameter.
- Lab or field data is insufficient to build an empirical input PDF.
- Use available data to identify the range of the uncertain parameters.
- Their distribution is assumed uniform within this range.

Entrainment parameters

- Model uses 2 entrainment coefficients.
- One entrainment parameter is perturbed using the upper and lower bound of Bhaumik's experiment.
- The other one is perturbed by around 20% of its experimental best match value.

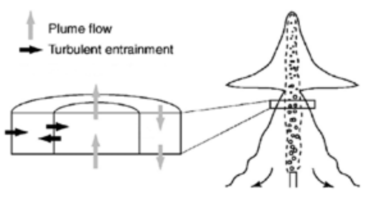

Figure 3 : Modified from Crounse et al., 2007

Characterizing the uncertain parameters

Flow rate

- Initial estimate: 5,000 barrels/day (NOAA, April 28) satellite images;
- Posterior estimate: 50,000-70,000 barrels/day (McNutt et al. 2012). in-situ measurements;
- We designed different experiments to account for different flow rate uncertainties.

Figure 4 : McNutt et al. 2012

Characterizing the uncertain parameters

Flow rate

- Initial estimate: 5,000 barrels/day (NOAA, April 28) satellite images;
- Posterior estimate: 50,000-70,000 barrels/day (McNutt et al. 2012). in-situ measurements;
- We designed different experiments to account for different flow rate uncertainties.

Figure 4 : McNutt et al. 2012

Gas-to-oil ratio (GOR)

- Unit: volumn/volumn = $ft^3/barrel$ (at standard conditions).
- Reddy et al. (2012): 1600 $ft^3/barrel$, 2470 $ft^3/barrel$; Valentine et al. (2010): 3000 $ft^3/barrel$; McNutt et al. (2012): 1400-2400 $ft^3/barrel$.

Figure 5 : Reddy et al. 2012

Characterizing the uncertain parameters

Bubble/droplet size distribution

Two-parameter Rosin-Rammler distribution (Johansen et al. 2001, 2013):

$$V(d) = 1 - \exp[-k(d/d_{95})^n]$$

- 95^{th} percentile of the droplet size (d_{95}): 1-10mm (Johansen et al. 2003; Board and Others, 2005).
- Distributional spreading parameter (n): 1.5-4 (Lefebvre, 1988).

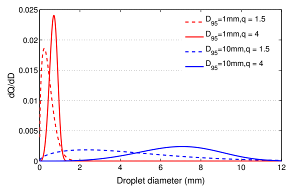

Figure 6 : Examples of droplet size distribution

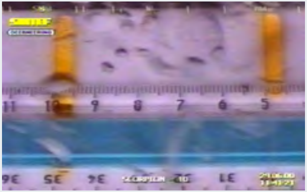

Figure 7 : Johansen et al. 2001

Deepwater Horizon experiments

Parameter	5d experiment	6d experiment1	6d experiment2
Entrainment coefficient[a]	$(0.06, 0.116)$	$(0.06, 0.116)$	$(0.06, 0.116)$
Entrainment ratio[b]	$(0.4, 0.6)$	$(0.4, 0.6)$	$(0.4, 0.6)$
Gas-to-oil ratio[c]	$(1400, 3000)$	$(1400, 3000)$	$(1400, 3000)$
95th percentile of the droplet size (d_{95})[d]	$(1, 10)$	$(1, 10)$	$(1, 10)$
Droplet distribution spreading ratio[e]	$(1.5, 4)$	$(1.5, 4)$	$(1.5, 4)$
Flow rate	60000	(5000,60000)	(50000,70000)

Table 2 : Uncertain input variables and their initial distributions. [a] Entrainment coefficient range from Bhaumik (2005). [b] Entrainment ratio range from Bhaumik (2005). [c] Gas-to-oil ratio ($ft^3/barral$) range from Reddy et al. (2012) and Valentine et al. (2010). [d] 95th percentile of the droplet size (d_{95}) (mm) range from Johansen et al. (2000). [e] Droplet distribution spreading ratio range from Lefebvre (1988).

Deepwater Horizon experiments

Parameter	5d experiment	6d experiment1	6d experiment2
Entrainment coefficient[a]	(0.06, 0.116)	(0.06, 0.116)	(0.06, 0.116)
Entrainment ratio[b]	(0.4, 0.6)	(0.4, 0.6)	(0.4, 0.6)
Gas-to-oil ratio[c]	(1400, 3000)	(1400, 3000)	(1400, 3000)
95th percentile of the droplet size (d_{95})[d]	(1, 10)	(1, 10)	(1, 10)
Droplet distribution spreading ratio[e]	(1.5, 4)	(1.5, 4)	(1.5, 4)
Flow rate	60000	(5000,60000)	(50000,70000)

Table 2 : Uncertain input variables and their initial distributions. [a] Entrainment coefficient range from Bhaumik (2005). [b] Entrainment ratio range from Bhaumik (2005). [c] Gas-to-oil ratio ($ft^3/barral$) range from Reddy et al. (2012) and Valentine et al. (2010). [d] 95th percentile of the droplet size (d_{95}) (mm) range from Johansen et al. (2000). [e] Droplet distribution spreading ratio range from Lefebvre (1988).

- Uncertain parameter space is 5 (or 6)-dimensional.
- Monte-Carlo(MC) sampling is traditionally used to explore all possible inputs and to calculate the ensuing statistics such as mean and standard deviation.
- MC requires a very large sample size and can be computationally challenging.
- Modern UQ relies on a model proxy to perform the statistics.

Outline

Proxy methods

Main idea

- **Indirect sampling:** Use a small ensemble to build a faithful proxy for the model and use it to estimate the model statistics.

Proxy methods

Main idea

- **Indirect sampling:** Use a small ensemble to build a faithful proxy for the model and use it to estimate the model statistics.

Polynomial Chaos Expansion

Let $u(z, \boldsymbol{\xi})$ be the model output (trap/peel height, gas mass flux) that depends on space z and the uncertain input varible $\boldsymbol{\xi}$. It can be approximated using a truncated ***Polynomial Chaos Expansion*** **(*PCE*)** :

$$u(z, \boldsymbol{\xi}) \approx u_P(z, \boldsymbol{\xi}) = \sum_{n=0}^{P} \hat{u}_n(z)\psi_n(\boldsymbol{\xi})$$

where $\boldsymbol{\xi}$ is a 5/6-dimensional random vector, $\hat{u}_n(z)$ are the expansion coefficients, and $\psi_n(\boldsymbol{\xi})$ are suitably chosen basis functions.

- Determine the expansion coefficients
- PC basis selection

Determine the PC coefficients

Minimize $\epsilon = u - u_p$ (ensemble-based)

Determine the PC coefficients

Minimize $\epsilon = u - u_p$ (ensemble-based)

Projection: minimize $||u - u_p||_2^2 = \int (u - u_p)^2 \rho(\boldsymbol{\xi}) \mathrm{d}\boldsymbol{\xi}$

$$\hat{u}_n = \frac{\langle u, \psi_n \rangle}{\langle \psi_n, \psi_n \rangle}, \; n = 0, 1, 2, \ldots, P$$

$$\langle u, \psi_n \rangle = \int \psi_n(\boldsymbol{\xi})\, u(\boldsymbol{\xi})\, p(\boldsymbol{\xi})\, \mathrm{d}\boldsymbol{\xi} \qquad \text{(Quadrature rules)}$$

Determine the PC coefficients

Minimize $\epsilon = u - u_p$ (ensemble-based)

Projection: minimize $||u - u_p||_2^2 = \int (u - u_p)^2 \rho(\boldsymbol{\xi}) \mathrm{d}\boldsymbol{\xi}$

$$\hat{u}_n = \frac{\langle u, \psi_n \rangle}{\langle \psi_n, \psi_n \rangle}, \; n = 0, 1, 2, \ldots, P$$

$$\langle u, \psi_n \rangle = \int \psi_n(\boldsymbol{\xi}) \, u(\boldsymbol{\xi}) \, p(\boldsymbol{\xi}) \, \mathrm{d}\boldsymbol{\xi} \qquad \text{(Quadrature rules)}$$

Regression: minimize $||u - u_p||_2^2 = \sum_{s=1}^{S} (u(\xi_s) - u_p(\xi_s))^2$

$$u(\boldsymbol{\xi}) = \sum_{n=0}^{P} \hat{u}_n \psi_n(\boldsymbol{\xi}) \text{ or in matrix form } \boldsymbol{\Psi} \hat{\boldsymbol{u}} = \boldsymbol{u}$$

$$\hat{\boldsymbol{u}} = \left(\boldsymbol{\Psi}^\top \boldsymbol{\Psi} \right)^{-1} \boldsymbol{\Psi}^\top \boldsymbol{u}$$

Determine the PC coefficients

Minimize $\epsilon = u - u_p$ (ensemble-based)

Projection: minimize $||u - u_p||_2^2 = \int (u - u_p)^2 \rho(\boldsymbol{\xi}) \mathrm{d}\boldsymbol{\xi}$

$$\hat{u}_n = \frac{\langle u, \psi_n \rangle}{\langle \psi_n, \psi_n \rangle}, \quad n = 0, 1, 2, \ldots, P$$

$$\langle u, \psi_n \rangle = \int \psi_n(\boldsymbol{\xi}) \, u(\boldsymbol{\xi}) \, p(\boldsymbol{\xi}) \, \mathrm{d}\boldsymbol{\xi} \qquad \text{(Quadrature rules)}$$

Regression: minimize $||u - u_p||_2^2 = \sum_{s=1}^{S} (u(\xi_s) - u_p(\xi_s))^2$

$$u(\boldsymbol{\xi}) = \sum_{n=0}^{P} \hat{u}_n \psi_n(\boldsymbol{\xi}) \text{ or in matrix form } \boldsymbol{\Psi}\hat{\boldsymbol{u}} = \boldsymbol{u}$$

$$\hat{\boldsymbol{u}} = \left(\boldsymbol{\Psi}^\top \boldsymbol{\Psi}\right)^{-1} \boldsymbol{\Psi}^\top \boldsymbol{u}$$

Basis Pursuit Denoising (BPDN): Add sparsity requirement

$$\min \ ||\hat{\boldsymbol{u}}||_1 \ \text{ subject to } \ ||\boldsymbol{u} - \boldsymbol{u_p}||_2^2 \leq \sigma \qquad \text{where} ||\hat{u}||_1 = \sum_{k=o}^{P} |u_k|$$

A first exploration of the parameter space

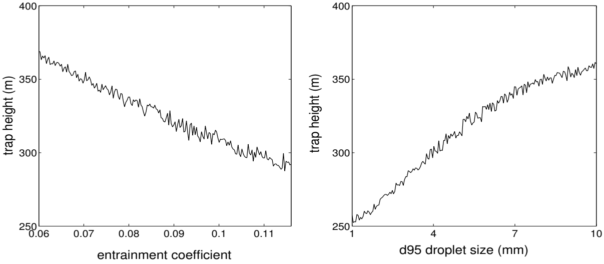

Figure 8 : Trap height response curves obtained with direct sampling along the central axes of uncertain space.

- Model noise. ⇒ negligible from a practical point of view.
- Low order polynomials should be able to capture the trend if not the noise. ⇒ 5-th order PC basis.
- Different PC approaches: PC-projection (require 903 realizations); PC-regression (require 504 realizations); PC-BPDN (require 100 realizations).
- A 50,000 MC set is generated for verification purpose.

Outline

1D comparision

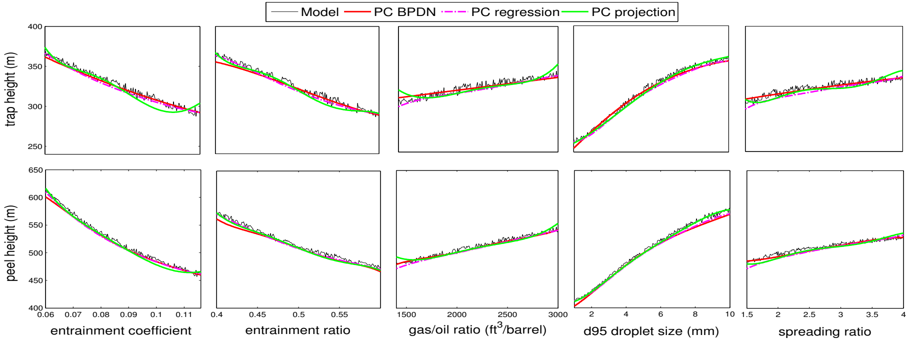

Figure 9 : 1D comparison of proxy methods and model simulations

- Most proxy-based response curves agree with the validation curve except that the proxy-based responses are oscillation-free.
- PC-projection shows more oscillatory features.

Error metrics

We use two error measures to compare different proxies.

Global measure: normalized Root Mean Square Error (nRMSE)

$$nRMSE = \frac{(\sum |\boldsymbol{u}_{MC} - \boldsymbol{u}_{proxy}|^2)^{1/2}}{(\sum |\boldsymbol{u}_{MC}|^2)^{1/2}}$$

Proxy method	Trap height nRMSE	Peel height nRMSE
PC-projection	0.0509	0.0267
PC-regression	0.0177	0.0097
PC-BPDN	0.0195	0.0152

Table 3 : nRMSE for trap height and peel height.

- PC-projection exhibits the largest error; other methods perform similarly.

Statistical measure: error 95

Local relative error can be defined as:

$$\epsilon = \frac{|\boldsymbol{u}_{MC} - \boldsymbol{u}_{proxy}|}{max(\boldsymbol{u}_{MC}) - min(\boldsymbol{u}_{MC})}$$

Error 95 is defined as the error at which the cumulative density function reaches 95%.

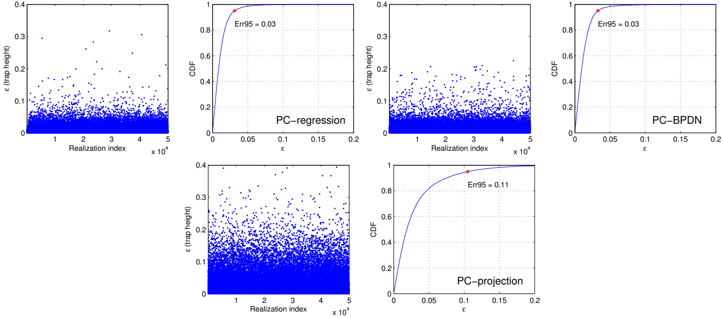

Figure 10 : Trap height local relative errors and error 95 using PC-regression, PC-BPDN and PC-projection, respectively.

- PC-projection underperforms in the presence of noise.
- The local errors are relatively small using PC-BPDN.

MC Reference PDF

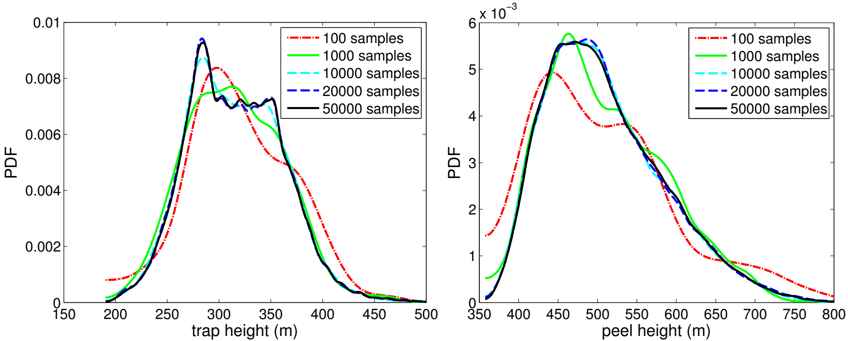

Figure 11 : The PDFs of trap height and peel height with different size of LHS ensemble.

- The shape of the PDF changes little once sample size exceeds 20,000. The 50,000 MC set will be our reference PDF.
- The trap height MC-PDF exhibits a narrow mode at 275 meter and a broad shoulder.
- The peel height MC-PDF exhibits a broad peek between 450-500m.

Comparisons of proxy-based PDFs

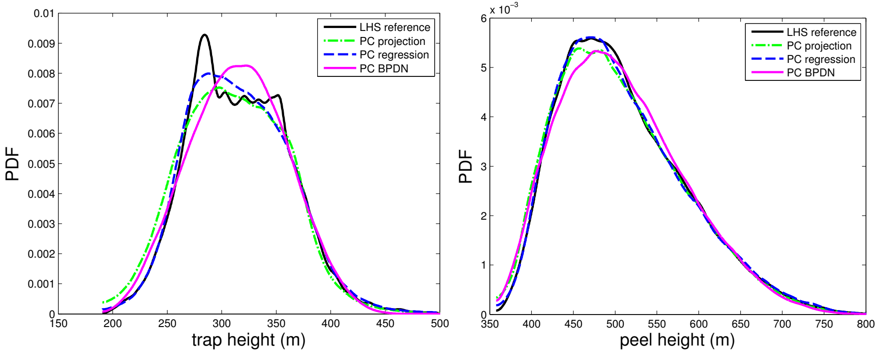

Figure 12 : Comparisons of trap height and peel height PDFs obtained from different proxies with the reference MC-PDF.

- The mode and spread of the peel height PDF using proxies agree well with the MC reference.
- The mode of the trap height PDF is not well captured.

Outline

Trap height PDF

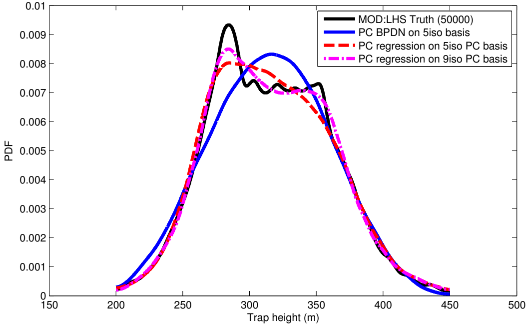

Figure 13 : Trap height PDF with different PC basis and different ensemble sizes.

Three experiments:

Ensemble	PC basis
100	252
504	252
4004	2002

nRMSE	Error 95
0.0195	0.0327
0.0178	0.0311
0.0249	0.0354

- Sampling errors (increase the ensemble size)? proxy errors (use larger basis)? Combination of both (do both)?
- Relative entropy $= \sum_i p(i) ln \frac{p(i)}{q(i)}$ 0.1084 0.0276 0.0125

Sensitivity analysis

Analysis of variance

Analyzing the respective contributions of each parameter to the variance of the output.

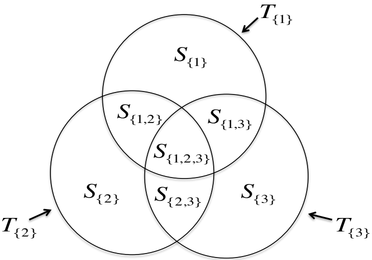

Sensitivity analysis

Analysis of variance

Analyzing the respective contributions of each parameter to the variance of the output.

Approach

The sensitivity indices are defined as:

$$S_{i_1\ldots i_s}(u) = \frac{V[u_{i_1\ldots i_s}]}{V[u]}$$

which gives a fraction of the variance due to the combination of a set of parameters $(\xi_{i_1}, \ldots, \xi_{i_s})$.

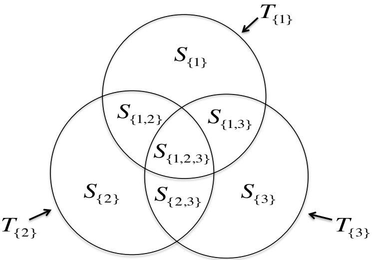

Sensitivity analysis

Analysis of variance

Analyzing the respective contributions of each parameter to the variance of the output.

Approach

The sensitivity indices are defined as:

$$S_{i_1\ldots i_s}(u) = \frac{V[u_{i_1\ldots i_s}]}{V[u]}$$

which gives a fraction of the variance due to the combination of a set of parameters $(\xi_{i_1}, \ldots, \xi_{i_s})$.

Properties of sensitivity indices

$\sum S_{\mathrm{i}} = 1,$ sensitivity indices

$\sum S_{\{i\}} \leq 1,$ 1st-order sensitivity indices

$\sum T_{\{i\}} \geq 1,$ total-order sensitivity indices

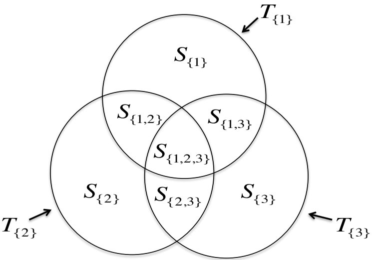

Sensitivity analysis

Analysis of variance

Analyzing the respective contributions of each parameter to the variance of the output.

Approach

The sensitivity indices are defined as:

$$S_{i_1 \dots i_s}(u) = \frac{V[u_{i_1 \dots i_s}]}{V[u]}$$

which gives a fraction of the variance due to the combination of a set of parameters $(\xi_{i_1}, \dots, \xi_{i_s})$.

Properties of sensitivity indices

$\sum S_{\mathrm{i}} = 1,$ sensitivity indices

$\sum S_{\{i\}} \leq 1,$ 1st-order sensitivity indices

$\sum T_{\{i\}} \geq 1,$ total-order sensitivity indices

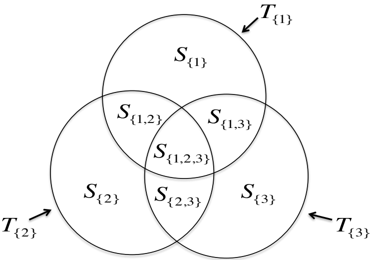

Sensitivity analysis

Analysis of variance

Analyzing the respective contributions of each parameter to the variance of the output.

Approach

The sensitivity indices are defined as:

$$S_{i_1 \ldots i_s}(u) = \frac{V[u_{i_1 \ldots i_s}]}{V[u]}$$

which gives a fraction of the variance due to the combination of a set of parameters $(\xi_{i_1}, \ldots, \xi_{i_s})$.

Properties of sensitivity indices

$\sum S_i = 1,$ sensitivity indices

$\sum S_{\{i\}} \leq 1,$ 1st-order sensitivity indices

$\sum T_{\{i\}} \geq 1,$ total-order sensitivity indices

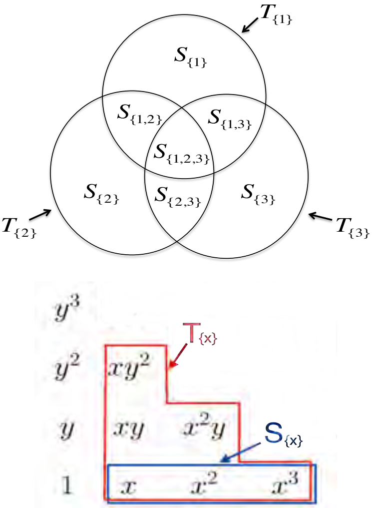

Figure 14 : Illustration of different sensitivity indices.

Comparison of sensitivity indices

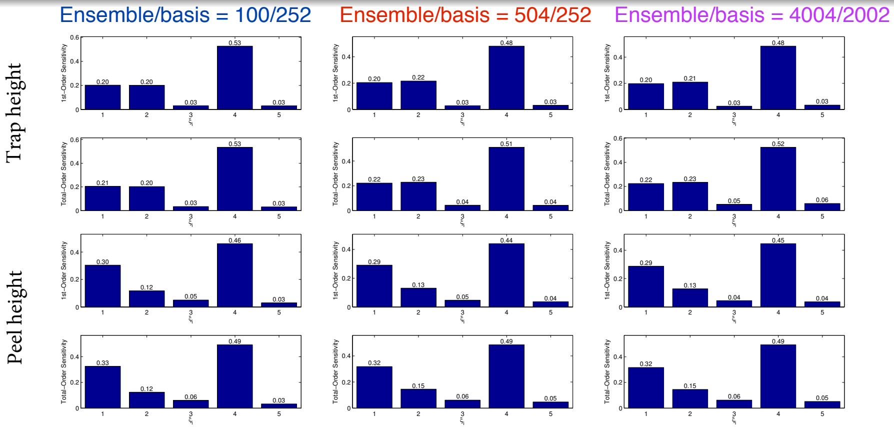

Figure 15 : 1st-order and total-order sensitivity indices for trap height (top) and peel height (bottom). Proxies are from the previous three experiments.

- Reliable sensitivity indices can be obtained using PCE with low order PC basis and small ensemble size.

Conclusion remarks

- Proxy methods make the UQ analysis possible during emergency response. Various analysis show that they are able to explore the parameter space with acceptable fidelity.

Conclusion remarks

- Proxy methods make the UQ analysis possible during emergency response. Various analysis show that they are able to explore the parameter space with acceptable fidelity.
- PC-BPDN provides a decent approach as it reduces the size of the ensemble and allows model noise. Also, PC method lends itself to a straightforward sensitivity analysis.

Conclusion remarks

- Proxy methods make the UQ analysis possible during emergency response. Various analysis show that they are able to explore the parameter space with acceptable fidelity.
- PC-BPDN provides a decent approach as it reduces the size of the ensemble and allows model noise. Also, PC method lends itself to a straightforward sensitivity analysis.
- Although the mode of trap height is not well captured using only 100 MC samples, the spread of the trap height and sensitivity indices are quite reliable.

Outline

5D experiments

Parameter	5d experiment	6d experiment1	6d experiment2
Entrainment coefficient	$(0.06, 0.116)$	$(0.06, 0.116)$	$(0.06, 0.116)$
Entrainment ratio	$(0.4, 0.6)$	$(0.4, 0.6)$	$(0.4, 0.6)$
Gas-to-oil ratio	$(1400, 3000)$	$(1400, 3000)$	$(1400, 3000)$
95th percentile of the droplet size (d_{95})	$(1, 10)$	$(1, 10)$	$(1, 10)$
Droplet distribution spreading ratio	$(1.5, 4)$	$(1.5, 4)$	$(1.5, 4)$
Flow rate	60000	(5000,60000)	(50000,70000)

Table 4 : Uncertain input variables and their initial distributions.

- 5^{th} order isotropic truncation PC basis (contains 252 polynomials) is used in this experiment.
- The proxy we used for this part is PC-BPDN and the ensemble size is 100.

Trap/peel height PDF

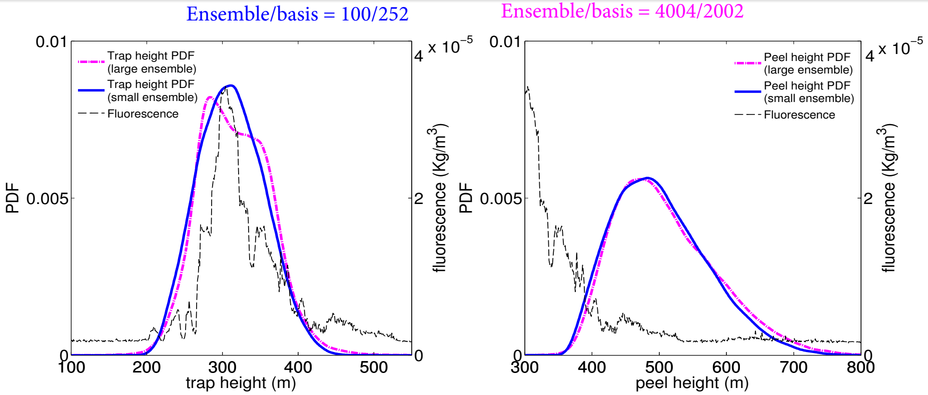

Figure 16 : Trap height PDF produced by PC proxy (large ensemble) with 100,000 samples, Trap height PDF produced by PC proxy (small ensemble) with 100,000 samples, Fluorescence measurement, a proxy for oil concentration.

- Fluorescence intensity can be regarded as a measure of oil concentration.
- The observations fall within the envelop of the estimated PDF.

Outline

Mass dissolution in depth

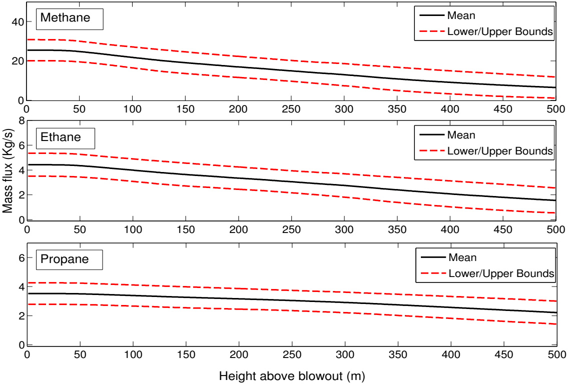

Figure 17 : Mean and standard deviation of gas mass fluxes associated different gas components for the first 500 meters of blowout.

- Gas mass fluxes do not dissolve completely at the trap height.
  $\Rightarrow$ about 50% of methane escapes the lowest intrusion.
- Including gas into the far-field model is necessary.

Gas mass flux PDF

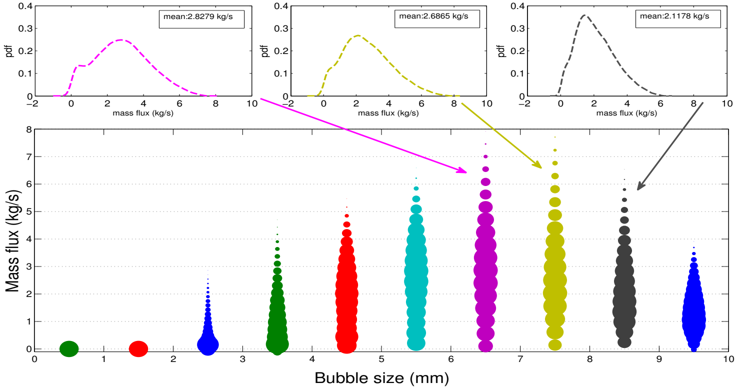

Figure 18 : Mass flux PDF at the trap height for different gas bubble sizes. Input for Lagrangian model - prediction with uncertainty.

- The distributional information of gas mass fluxes can be passed into the next stage oil fate model.
- Largest uncertainties remain in the droplet size range from 6 to 8 mm.

Outline

5D sensitivity

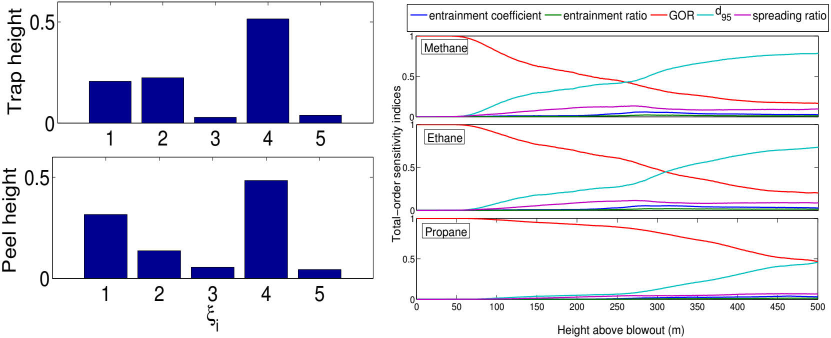

Figure 19 : Left: Total sensitivity indices for trap height/peel height. Right: Total sensitivity indices for methane, ethane and propane as a function of depth.

- The entrainment parameters and d_{95} have the highest sensitivity indices for trap/peel height.
- GOR dominates first stage of gas mass fluxes; d_{95} dominates the latter stage.

Outline

6D experiments

Parameter	5d experiment	6d experiment1	6d experiment2
Entrainment coefficient	$(0.06, 0.116)$	$(0.06, 0.116)$	$(0.06, 0.116)$
Entrainment ratio	$(0.4, 0.6)$	$(0.4, 0.6)$	$(0.4, 0.6)$
Gas-to-oil ratio	$(1400, 3000)$	$(1400, 3000)$	$(1400, 3000)$
95th percentile of the droplet size (d_{95})	$(1, 10)$	$(1, 10)$	$(1, 10)$
Droplet distribution spreading ratio	$(1.5, 4)$	$(1.5, 4)$	$(1.5, 4)$
Flow rate	60000	(5000,60000)	(50000,70000)

Table 5 : Uncertain input variables and their initial distributions.

- 5^{th} order isotropic truncation PC basis (contains 462 polynomials) is used in these two experiments.
- The proxy we used here is PC-BPDN and the ensemble size is 200.
- An independent database consisting of 2,000 member MC ensemble is generated to verify the accuracy of the proxy.

Trap height and peel height error metrics

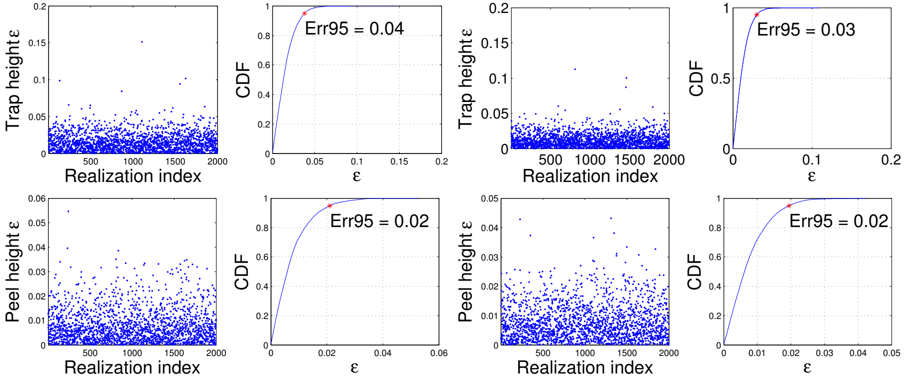

Figure 21 : Local errors and error 95 for trap height and peel height in 6D experiment1 (left) and 6D experiment2 (right).

- The error 95 for trap height and peel height are less than 4%.

Gas mass fluxes error metrics

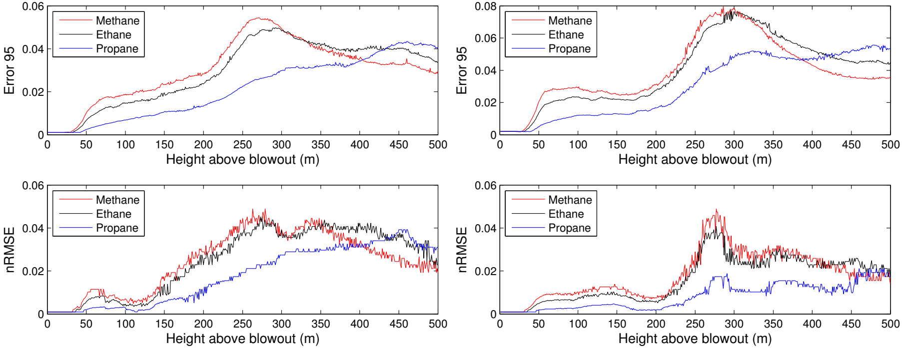

Figure 22 : Error 95 and nRMSE for methane, ethane and propane gas mass fluxes in two 6d experiments. Left: Gas mass fluxes error metrics in experiment1. Right: Gas mass fluxes error metrics in experiment2.

- The global error measure and the statistical error measure confirms the fidelity of the proxy method.

Trap height PDF

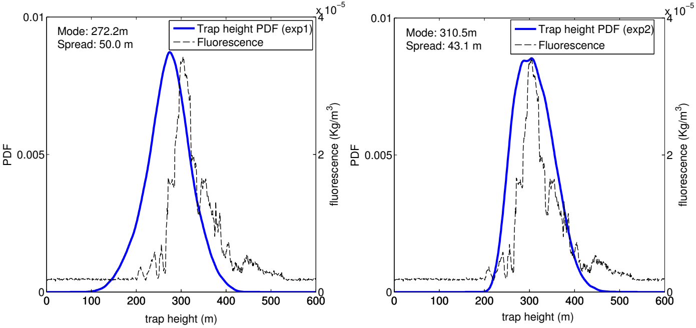

Figure 23 : Comparison of trap height PDF and the fluorescence measurement. The red curve is the trap height PDF and the blue curve is the fluorescence measurement. Left: experiment1; Right: experiment2.

- Fluorescence measurements fall off the peak of the estimated trap height PDF in experiment 1.
- The spreads of both experiments are similar.
  $\Rightarrow$ trap height spread is not sensitive to the perturbation range.

Sensitivity indices

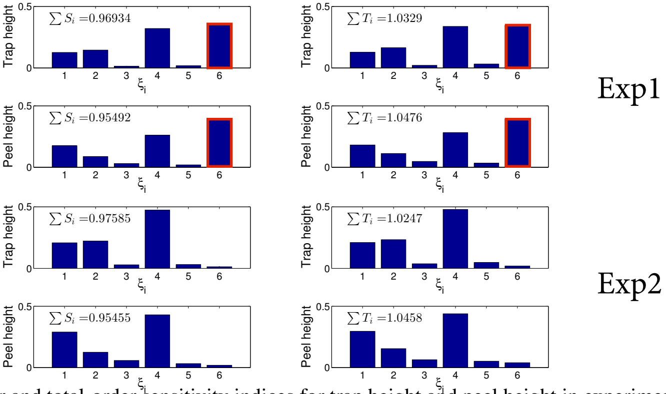

Figure 24 : 1st-order and total-order sensitivity indices for trap height and peel height in experiment1 (top) and experiment2 (bottom).

- Flow rate is dominant in experiment1 but not in experiment2.
- Entrainment parameters and d_{95} have huge impact in both experiments.
- The coupling between uncertain inputs are weak.

Sensitivity indices

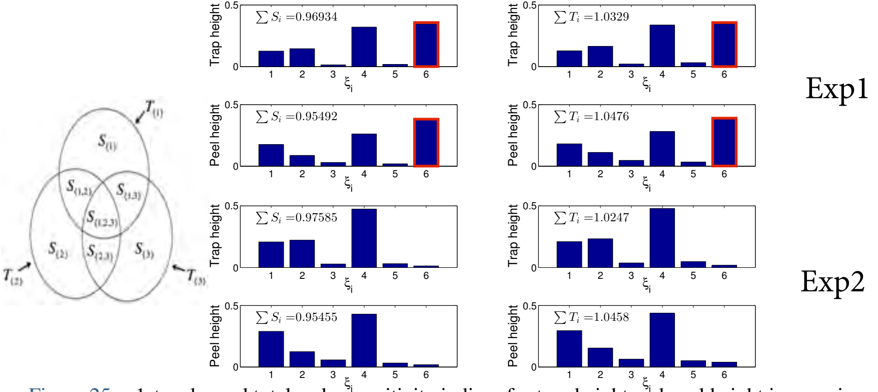

Figure 25 : 1st-order and total-order sensitivity indices for trap height and peel height in experiment1 (top) and experiment2 (bottom).

- Flow rate is dominant in experiment1 but not in experiment2.
- Entrainment parameters and d_{95} have huge impact in both experiments.
- The coupling between uncertain inputs are weak.

Gas mass fluxes sensitivity indices

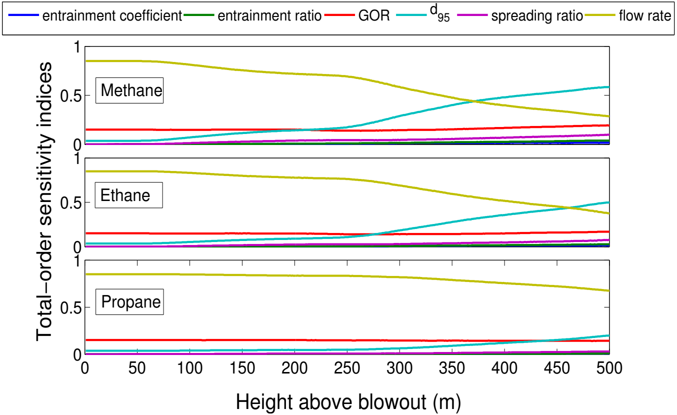

Figure 26 : Evolution of the total sensitivity indices for mass flux of methane, ethane and propane associated with different uncertain input variables in experimen1.

- Flow rate is dominant at the initial stage.
- d_{95} becomes clearly dominant as the plume rises.

Gas mass fluxes sensitivity indices

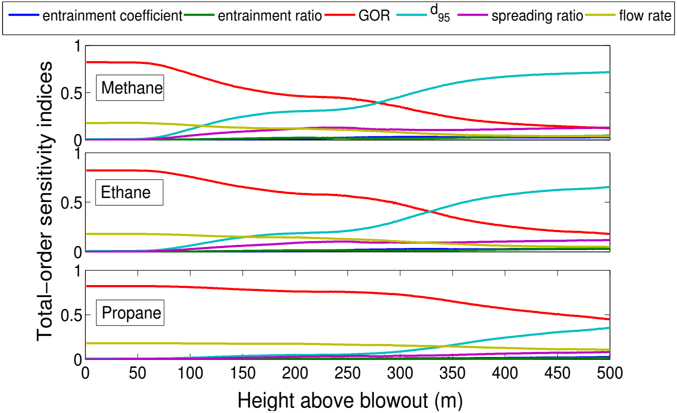

Figure 27 : Evolution of the total sensitivity indices for mass flux of methane, ethane and propane associated with different uncertain input variables in experiment2.

- GOR is dominant at the initial stage; flow rate also shows a contribution at the beginning.
- d_{95} becomes clearly dominant as the plume rises.

Conclusion remarks

- A qualitative agreement between the model and observation is established: the observations fall within the envelop of the estimated PDF.
- The natural gases do not dissolve completely at the subsurface intrusion level. Therefore, it is necessary to include gas into the far-field model.
- Entrainment parameters and d_{95} are the largest contributors to the trap height and peel height uncertainties. Flow rate and GOR are the dominant contributors to the gas mass flux uncertainty at the near well head region and d_{95} is the largest contributor for the gas mass flux uncertainty at the further region.

Summary

- Proxy-type methods are used to propagate the uncertainty and perform sensitivity analysis.

Summary

- Proxy-type methods are used to propagate the uncertainty and perform sensitivity analysis.
- Polynomial Chaos with compressive sensing is used in the experiments because of three advantages: accounting for model error, sparse representation, straightforward sensitivity analysis.

Summary

- Proxy-type methods are used to propagate the uncertainty and perform sensitivity analysis.
- Polynomial Chaos with compressive sensing is used in the experiments because of three advantages: accounting for model error, sparse representation, straightforward sensitivity analysis.
- Various error metrics suggest that the proxies are able to predict statistical information with acceptable fidelity.

Summary

- Proxy-type methods are used to propagate the uncertainty and perform sensitivity analysis.
- Polynomial Chaos with compressive sensing is used in the experiments because of three advantages: accounting for model error, sparse representation, straightforward sensitivity analysis.
- Various error metrics suggest that the proxies are able to predict statistical information with acceptable fidelity.
- The huge uncertainty range for the flow rate leads to substantial uncertainties in the ensuing quantities of interest whereas constraining the range to reasonable values shifts the dominance to uncertainties in droplet size distribution and in entrainment parameters.

Acknowledgements

- Advisor: Mohamed Iskandarani
- Committee members: Ashwanth Srinivasan, Tamay Özgökmen
- UQ group: Carlisle Thacker, Rafael Gonçalves, Ashwanth Srinivasan and Matthieu Hénaff
- Whole class of fall 2012
- Family and friends ...

Appendix

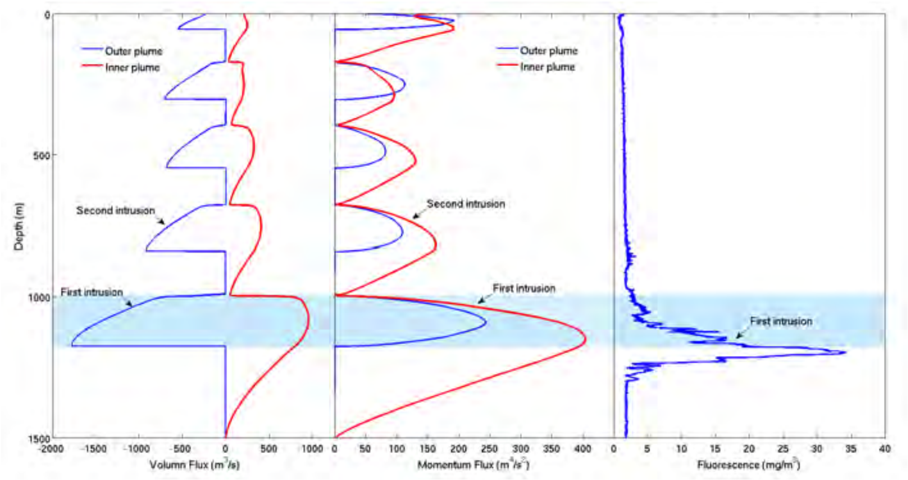

Outer plume
Inner plume
Second intrusion
First intrusion
Depth (m)
0
500
1000
1500
-2000
-1500
-1000
-500
0
500
1000
Volumn Flux (m^3/s)
0
50
100
150
200
250
300
350
400
Momentum Flux (m^4/s^2)
0
5
10
15
20
25
30
35
40
Fluorescence (mg/m^3)

Appendix

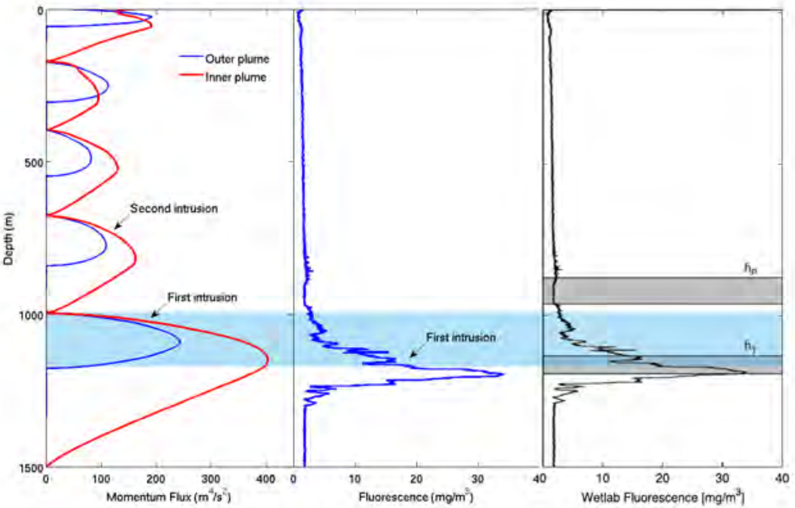

Outer plume
Inner plume
Second intrusion
First intrusion
Depth (m)
0
500
1000
1500
0 100 200 300 400
Momentum Flux (m^4/s^2)
0 10 20 30 40
Fluorescence (mg/m^3)
First intrusion
10 20 30 40
Wetlab Fluorescence [mg/m^3]
h_p
h_T

Appendix

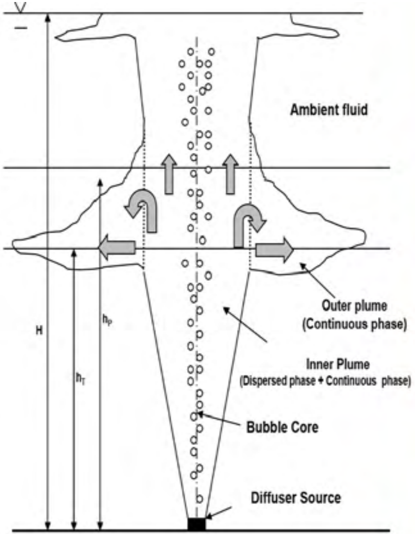
Ambient fluid
H
h_P
h_T
Outer plume
(Continuous phase)
Inner Plume
(Dispersed phase + Continuous phase)
Bubble Core
Diffuser Source

Appendix

Sampling method	Ensemble size	PC basis size	Truncation order
PC-projection	903	738[1]	(5,5,5,5,5)
PC-regression	504	252	(5,5,5,5,5)
PC-BPDN	100	252[2]	(5,5,5,5,5)
GPR	100		
MC	50,000		

Table 6 : The ensemble sizes used for different sampling methods.

[1]The pseudo-spectral scheme retains a larger number of polynomials than is possible with a total order truncation (contains 252 polynomials) using the same ensemble. The additional terms contained are the high order mixed terms disregarded by the traditional total order truncation.

[2]The numbers of non-zero PC coefficients determined using BPDN are 32 for trap height and 174 for peel height, respectively.